Electronic Supplementary Material (ESI) for Journal of Materials Chemistry A.

Supporting information

Biomass-derived C/N co-doped $Ni(OH)_2/Ni_xS_y$ with sandwich structure for supercapacitors

Yue Zhang, Lei Yu, Rudan Hu, Jianli Zhang, Yining Wang, Richao Niu, Xingyue Qian, Junwu Zhu*

Key Laboratory for Soft Chemistry and Functional Materials (Nanjing University of Science and Technology), Ministry of Education, Nanjing 210094, China.

** E-mail: zhujw@njust.edu.cn.*

Synthesis of reduced graphene oxide hydrogel (rGH)

The graphene oxide (GO) suspension was prepared according to the Hummers' method. Firstly, 1.5 mL GO suspension (5 mg g^{-1}) was transformed into glass tube. Then five tubes were transformed into the 100 mL Teflon-lined autoclave containing 13 mL deionized water and maintained at 150 °C for 12 h. After the autoclave naturally cooled down to room temperature, the obtained rGH was immersed into distilled water for dialysis.

Synthesis of C/N co-doped nickel sulfides with different ratio of egg white to nickel nitrate

This synthesis process is the same as the preparation of C/N-Ni_xS_y, and the only difference is the proportions of raw materials. The feeding mass of egg white is 13 g. According to the different mass of nickel nitrate: 0.10, 0.12, 0.14, 0.2, 0.24, and 0. 26 g, these obtained products are donated as C/N-Ni_xS_y-1, C/N-Ni_xS_y-2, C/N-Ni_xS_y-3, C/N-Ni_xS_y-4, C/N-Ni_xS_y-5, and C/N-Ni_xS_y-6, respectively.

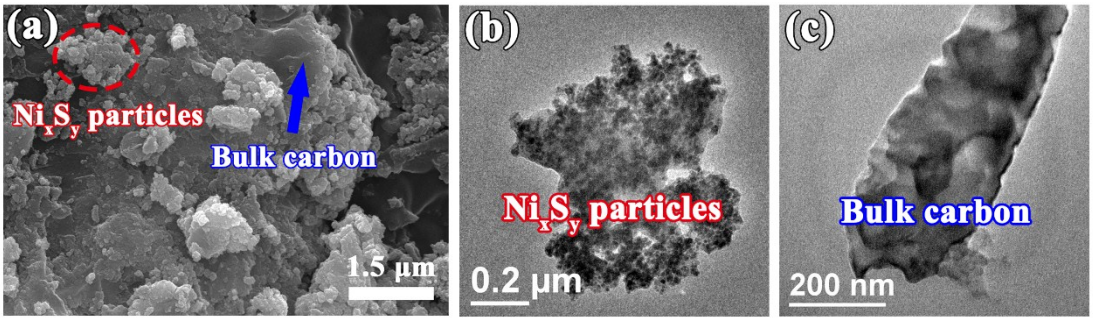

Fig. S1 (a) SEM images of C/N-Ni_xS_y, and TEM images of (b) Ni_xS_y nanoparticles and (c) bulk carbon in C/N-Ni_xS_y.

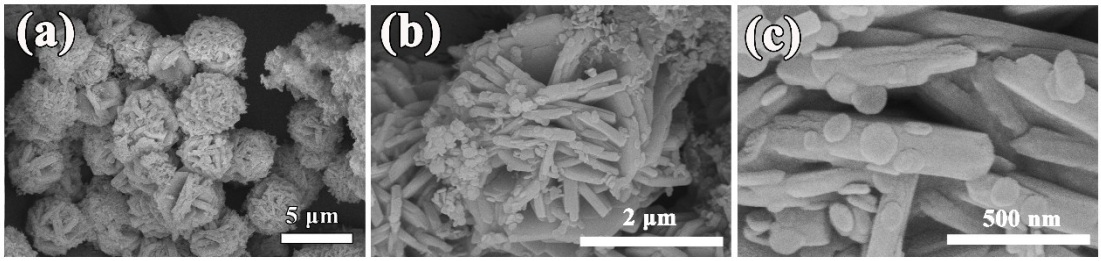

Fig. S2 SEM images of pure $Ni(OH)_2$.

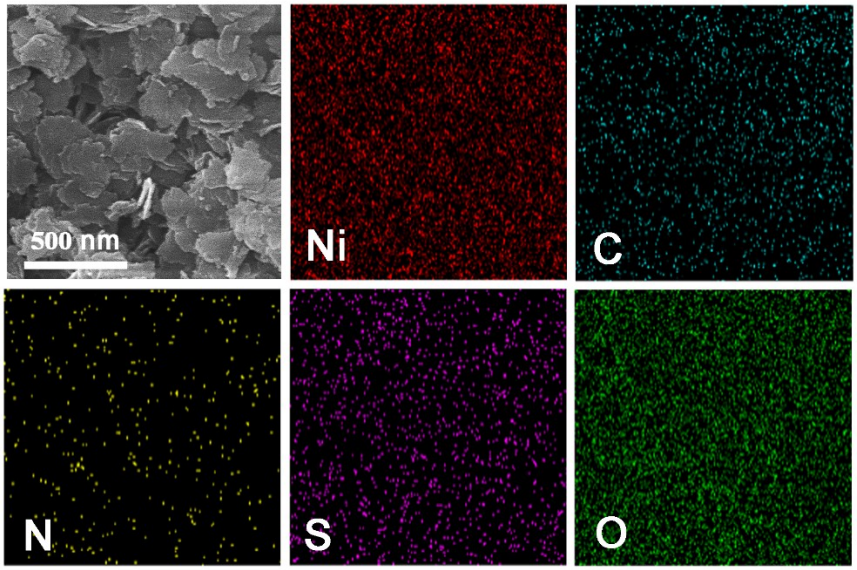

Fig. S3 SEM image and the corresponding EDX mapping images of Ni, S, C, N and O elements in C/N-$Ni(OH)_2$/Ni_xS_y.

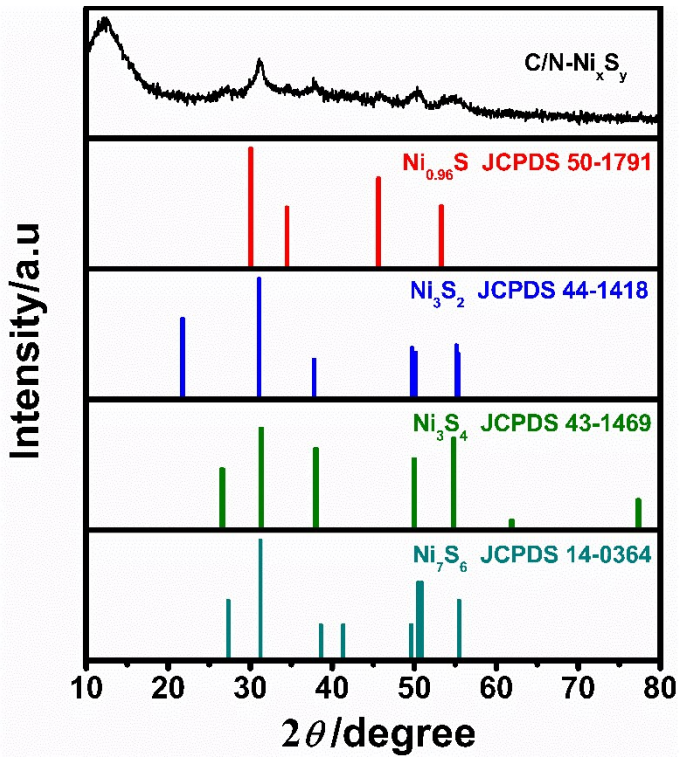

Fig. S4 XRD patterns of product C/N-Ni$_x$S$_y$.

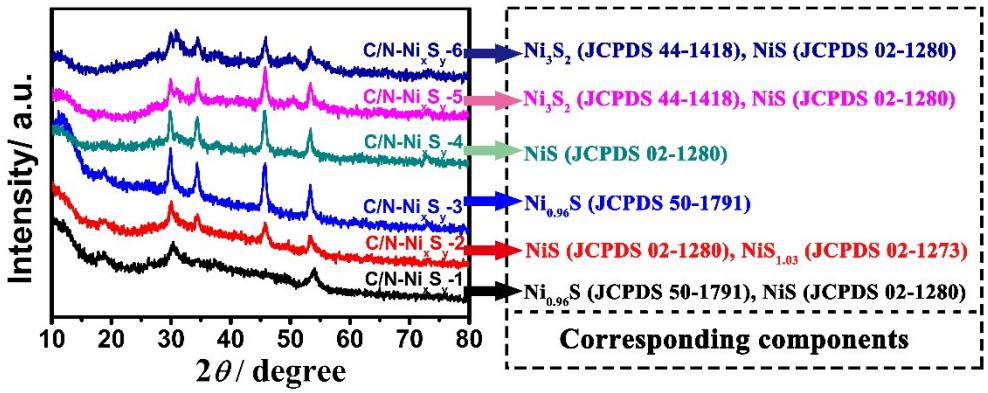

Fig. S5 XRD patterns of C/N-Ni$_x$S$_y$-1, C/N-Ni$_x$S$_y$-2, C/N-Ni$_x$S$_y$-3, C/N-Ni$_x$S$_y$-4, C/N-Ni$_x$S$_y$-5, and C/N-Ni$_x$S$_y$-6.

According to the XRD patterns of C/N-Ni$_x$S$_y$ and C/N-Ni$_x$S$_y$-1 to C/N-Ni$_x$S$_y$-6 (Fig. S3 and S4), the main components of products obtained without adding ammonia aqueous are Ni$_x$S$_y$. This result could further confirm that the egg white could be used as sulfur source to obtain Ni$_x$S$_y$.

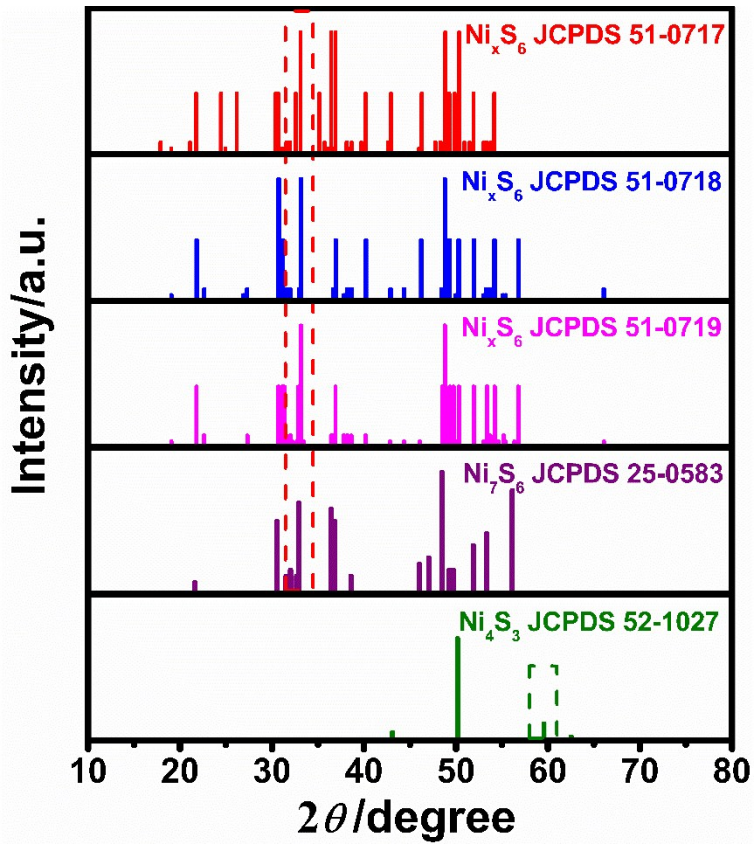

Fig. S6 Standard XRD patterns of Ni_xS_y in C/N-$Ni(OH)_2$/Ni_xS_y.

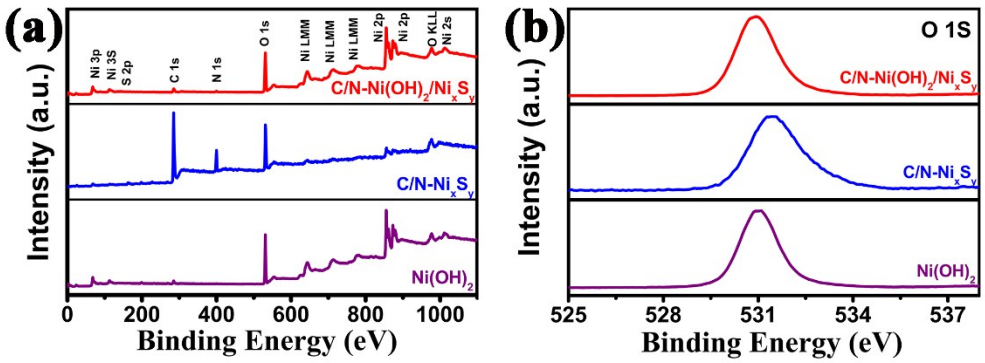

Fig. S7 XPS spectra of C/N-$Ni(OH)_2$/Ni_xS_y, C/N-Ni_xS_y, and $Ni(OH)_2$: (a) survey spectra, and (b) O 1S spectra.

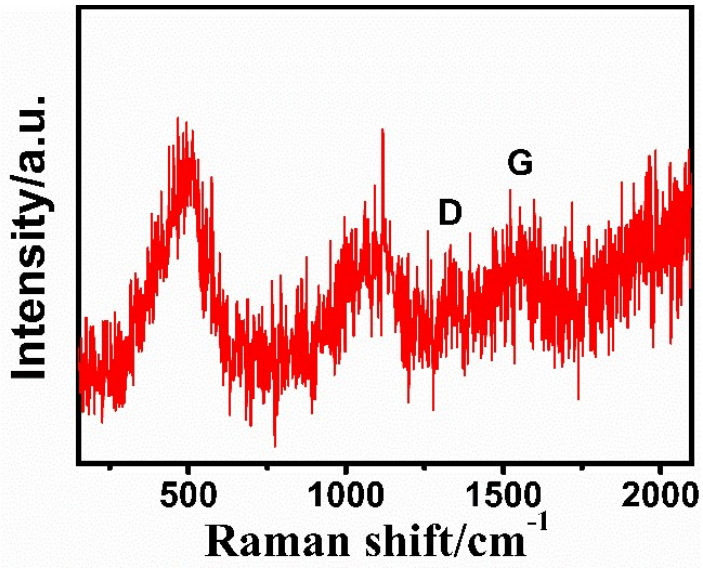

Fig. S8 Raman spectrum of C/N-$Ni(OH)_2$/Ni_xS_y composite.

As shown in Fig. S8, Raman spectrum was also measured to character the C/N-$Ni(OH)_2$/Ni_xS_y composite. The weak D and G bands can be observed, which attribute to A_{1g} vibration mode of disordered carbon and E_{2g} vibration mode of ordered graphitic carbon respectively, confirming the existence of carbon. Besides, the peaks around 509.1 and 1085.3 cm^{-1} could be attributed to nickel hydroxide, and the peak around 321 cm^{-1} could be attributed the presence of nickel sulfide. In general, both the XPS and Raman spectra further confirm the successfully C/N co-doping and the formation of $Ni(OH)_2$ and Ni_xS_y in C/N-$Ni(OH)_2$/Ni_xS_y.

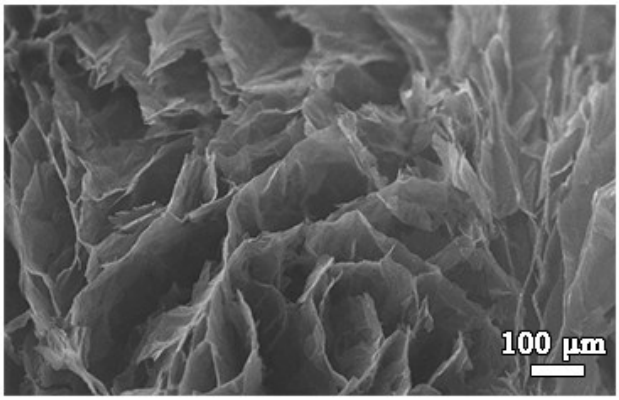

Fig. S9 SEM image of rGH.

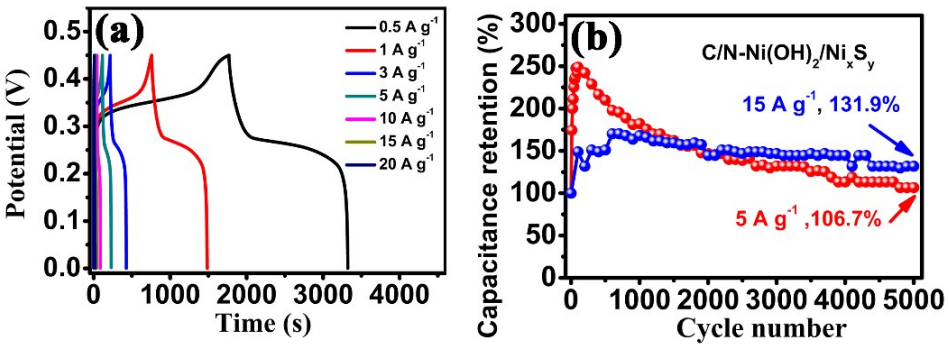

Fig. S10 (a) Galvanostatic charge-discharge curves and (b) cycling stability of C/N-$Ni(OH)_2/Ni_xS_y$ at different current densities.

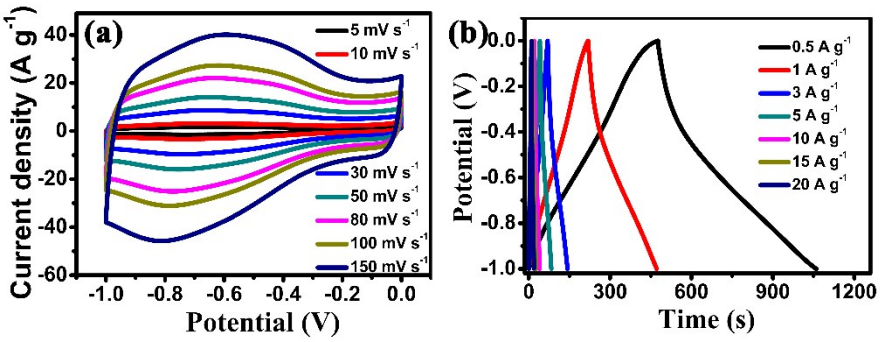

Fig. S11 (a) CV curves at different scan rates and (b) galvanostatic charge-discharge curves at different current densities of rGH.

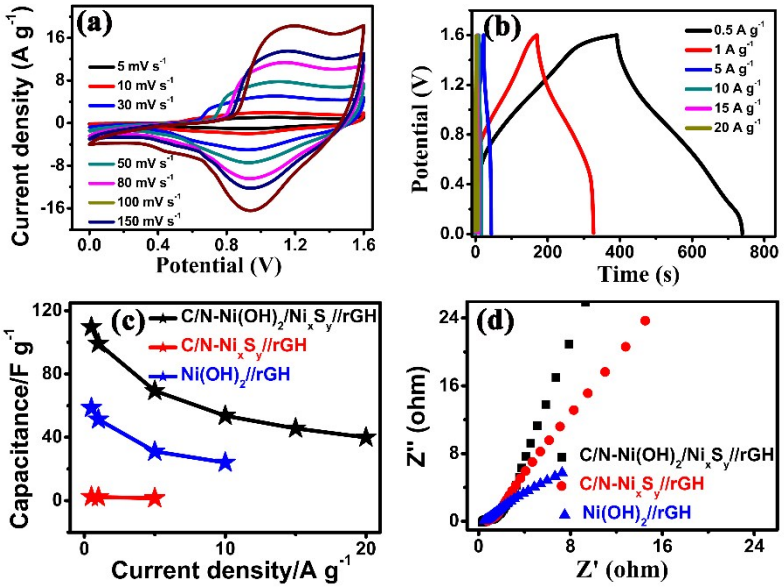

Fig. S12 (a) CV curves at different scan rates and (b) galvanostatic charge-discharge curves at different current densities of C/N-$Ni(OH)_2/Ni_xS_y$//rGH. (c) The capacitances at different current densities, and (d) Nyquist plots of C/N-$Ni(OH)_2/Ni_xS_y$//rGH, C/N-Ni_xS_y//rGH, and $Ni(OH)_2$//rGH.